Stomatal response to decreased relative humidity constrains the acceleration of terrestrial evapotranspiration

Xiao, Mingzhong

2020-09

Xiao , M , Yu , Z , Kong , D , Gu , X , Mammarella , I , Montagnani , L , Arain , M A , Merbold , L , Magliulo , V , Lohila , A , Buchmann , N , Wolf , S , Gharun , M , Hörtnagl , L , Beringer , J & Gioli , B 2020 , ' Stomatal response to decreased relative humidity constrains the acceleration of terrestrial evapotranspiration ' , Environmental Research Letters , vol. 15 , no. 9 , 094066 . https://doi.org/10.1088/1748-9326/ab9967

http://hdl.handle.net/10138/324390
https://doi.org/10.1088/1748-9326/ab9967

ENVIRONMENTAL RESEARCH
LETTERS

LETTER • **OPEN ACCESS**

Stomatal response to decreased relative humidity constrains the acceleration of terrestrial evapotranspiration

To cite this article: Mingzhong Xiao *et al* 2020 *Environ. Res. Lett.* **15** 094066

Environmental Research Letters

CrossMark

OPEN ACCESS

RECEIVED
12 December 2019

REVISED
19 May 2020

ACCEPTED FOR PUBLICATION
4 June 2020

PUBLISHED
27 August 2020

LETTER

Stomatal response to decreased relative humidity constrains the acceleration of terrestrial evapotranspiration

Mingzhong Xiao[1,2], Zhongbo Yu[1,2], Dongdong Kong[3], Xihui Gu[4], Ivan Mammarella[5], Leonardo Montagnani[6,7], M Altaf Arain[8], Lutz Merbold[9,10], Vincenzo Magliulo[11], Annalea Lohila[12], Nina Buchmann[10], Sebastian Wolf[10], Mana Gharun[10], Lukas Hörtnagl[10], Jason Beringer[13] and Beniamino Gioli[14]

1 State Key Laboratory of Hydrology-Water Resources and Hydraulic Engineering, Hohai University, Nanjing 210098, People's Republic of China
2 College of Hydrology and Water Resources, Hohai University, Nanjing 210098, People's Republic of China
3 Department of Water Resources and Environment, Sun Yat-sen University, Guangzhou 510275, People's Republic of China
4 Department of Atmospheric Science, School of Environmental Studies, China University of Geosciences, Wuhan 430074, People's Republic of China
5 Institute for Atmosphere and Earth System Research/Physics, Faculty of Science, University of Helsinki, PO Box 68, Finland
6 Faculty of Science and Technology, Free University of Bolzano, Universitätsplatz 5, Piazza Università, I-39100, Bolzano, Italy
7 Forest Services, Autonomous Province of Bolzano, Via Brennero 6, 39100, Bolzano, Italy
8 School of Geography and Earth Sciences and McMaster Centre for Climate Change, McMaster University, Hamilton, ON, Canada
9 Mazingira Centre, International Livestock Research Institute (ILRI), 00100, Nairobi, Kenya
10 Department of Environmental Systems Science, ETH Zurich, 8092, Zurich, Switzerland
11 Consiglio Nazionale delle Ricerche, Institute for Mediterranean Agricultural and Forest Systems, Via Patacca 85, 80056, Ercolano (Napoli), Italy
12 Finnish Meteorological Institute, Climate System Research, FIN-00101, Helsinki, Finland
13 School of Agriculture and Environment, University of Western Australia, Crawley 6009, Western Australia, Australia
14 Consiglio Nazionale delle Ricerche, Institute of Bioeconomy, via Giovanni Caproni 8, 50145, Firenze, Italy

E-mail: zyu@hhu.edu.cn and xmingzh@mail2.sysu.edu.cn

Keywords: terrestrial evapotranspiration, relative humidity, global warming, stomata regulation

Supplementary material for this article is available online

Abstract

Terrestrial evapotranspiration (ET) is thermodynamically expected to increase with increasing atmospheric temperature; however, the actual constraints on the intensification of ET remain uncertain due to a lack of direct observations. Based on the FLUXNET2015 Dataset, we found that relative humidity (RH) is a more important driver of ET than temperature. While actual ET decrease at reduced RH, potential ET increases, consistently with the complementary relationship (CR) framework stating that the fraction of energy not used for actual ET is dissipated as increased sensible heat flux that in turn increases potential ET. In this study, we proposed an improved CR formulation requiring no parameter calibration and assessed its reliability in estimating ET both at site-level with the FLUXNET2015 Dataset and at basin-level. Using the ERA-Interim meteorological dataset for 1979–2017 to calculate ET, we found that the global terrestrial ET showed an increasing trend until 1998, while the trend started to decline afterwards. Such decline was largely associated with a reduced RH, inducing water stress conditions that triggered stomatal closure to conserve water. For the first time, this study quantified the global-scale implications of changes in RH on terrestrial ET, indicating that the temperature-driven acceleration of the terrestrial water cycle will be likely constrained by terrestrial vegetation feedbacks.

1. Introduction

On a global scale, approximately two-thirds of the annual precipitation over land originates from terrestrial evapotranspiration (ET) (Oki and Kanae 2006). More than half of the total solar energy absorbed by the land surface is used as latent heat to sustain ET (Trenberth *et al* 2009). Detecting and attributing variations in terrestrial ET is therefore crucial for improving our understanding of land-atmosphere interactions and of the terrestrial water cycle, which is of key importance for water resource management, human activities, wellbeing and the associated carbon cycle (Wang and Dickinson 2012, Burke *et al* 2018).

In a changing climate, rising temperatures increase saturated water vapour pressure at a rate of approximately 6–7%K^{-1} according to the Clausius-Clapeyron equation. There is evidence of increasing water vapour content at both the surface and upper tropospheric levels (Trenberth *et al* 2005); thus, numerous previous studies have suggested surface relative humidity (RH: ratio of actual water vapour pressure to saturated water vapour pressure) to be constant (Dai 2006, Willett *et al* 2008). However, recent studies have indicated that the actual atmospheric water vapour content does not always increase at exactly the same rate as saturated vapour pressure. A sharp decrease in RH has been observed since 2000 from both gridded observational and reanalysis data (Simmons *et al* 2010, Willett *et al* 2014). Increasing evidence suggests that the decrease in terrestrial RH are due to the greater warming over land than the ocean (Byrne and O'Gorman 2016) and are associated with a concurrent decline in the soil moisture over vast regions in the terrestrial biosphere (Byrne and O'Gorman 2016, Zhou *et al* 2019). However, details about the patterns of reduced RH still remain unclear (Vicente-Serrano *et al* 2018).

Reduced RH implies increased vapour pressure deficit (VPD), which is an important proxy of atmospheric water demand by plants (Mcadam and Brodribb 2015, Yuan *et al* 2019). Intuitively, we expect that terrestrial evapotranspiration (ET) would increase with increased water demand; however, it has been well established that plants close their stomata to prevent excessive water loss in response to increasing atmospheric VPD (Mcadam and Brodribb 2015). Recent studies have highlighted that a rising VPD greatly limits terrestrial ET in many biomes through stomata regulation (Novick *et al* 2016, Rigden and Salvucci 2017). Using the ET estimated from the relative humidity at equilibrium (ETRHEQ) method, Rigden and Salvucci (2017) detected a sharp decline in ET from 1998 to 2014 in the continental United States, and they attributed this decrease mostly to the decline in stomatal conductance. However, large amounts of observational data, such as half-hourly vertical profiles of RH, are required to estimate the ETRHEQ, which limits its application.

Reduced RH generally decreases actual ET while increasing potential ET. This relationship is consistent with the complementary relationship (CR) framework between actual and potential ET stating that the fraction of energy not used for evapotranspiration is dissipated as increased sensible heat flux that in turn increases potential ET (Bouchet 1963). Because the CR framework of ET requires no detailed knowledge of the complex processes and interactions between soil, vegetation, and the near-surface atmosphere, CR-based approaches are easily deployable to directly estimate ET (Kahler and Brutsaert 2006, Szilagyi and Jozsa 2008, Huntington *et al* 2011, Brutsaert 2015). However, the application of CR-based methods was limited by the need of a local parameters calibration, while in this study we developed an improved CR formulation not requiring any calibration. Given that the global-scale constraints of changes in RH on terrestrial ET have not yet been quantified, the objectives of this study are (1) to develop a new method to estimate global terrestrial ET and verify its accuracy; (2) to detect and attribute the influences of changes in RH on terrestrial ET.

2. Methods and data

2.1. Observation data-based evaluation of the influence of RH on ET

Based on the observed ET, net radiation, surface air temperature, wind speed, and RH, data-driven approaches were established to evaluate the influence of RH on ET. A linear relationship between RH and ET was initially analyzed. To exclude the effects of net radiation, surface air temperature and wind speed, the partial correlation between observed RH and ET was calculated with the R package 'ppcor' (Kim 2015). Secondly, the relative importance of factors affecting ET was assessed to evaluate the contribution of RH to the variation in ET. With ET as predicted variable and net radiation, surface air temperature, wind speed, and RH as predictor variables, a multiple regression was built. The change in the coefficient of determination (R^2) when a predictor variable was removed from the multiple regression was calculated. The change in R^2 is also called partial R^2, and it represents the amount of unique variance that each predictor variable explains. Thereby, the partial R^2 in the multiple regression was used to illustrate the relative importance of factors affecting ET. Besides, the relative importance of factors affecting ET was further evaluated based on the permutation-based variable importance in a Random Forest method (Breiman 2001), as detailed in (Strobl *et al* 2007, Grömping 2009). The Random Forest method was implemented through the R package 'ranger' (Wright and Ziegler 2017). Half of the observed data was randomly selected as calibration data, while the other as verification data. The performances of the multiple regression method and the Random Forest method in estimating ET were evaluated using the metrics of R^2 and root mean square error (RMSE).

2.2. Estimation of actual ET by a theoretical derived method

We developed an improved complementary relationship (CR) formulation to estimate actual ET. The key idea behind the CR formulation is that as a surface dries, the fraction of energy not used for actual ET (ET_a) is dissipated as sensible heat flux that increases temperature and, hence, potential ET (ET_p), obtaining a complementary relationship between ET_a and ET_p (Bouchet 1963, Aminzadeh *et al* 2016). Implicit to the CR formulation, equilibrium ET (ET_w) is defined as the evaporation from an extensive well-watered surface where energy is the limiting factor. With limited water availability, the reduction in energy used for ET_a thus becomes available as sensible heat flux, thereby increasing ET_p. The CR formulation can be expressed as (Kahler and Brutsaert 2006):

$$ET_p - ET_w = b\,(ET_w - ET_a) \tag{1}$$

Therefore, ET_a can be estimated based on equation (1) as:

$$ET_a = \frac{(1+b)\,ET_w - ET_p}{b} \tag{2}$$

where b is a coefficient that depicts the proportion of sensible heat flux that increases ET_p and is calculated as follows (Granger 1989, Aminzadeh *et al* 2016):

$$b = \frac{1}{\gamma}\frac{e_s^* - e_w^*}{T_s - T_w} \tag{3}$$

where e_s^* is saturated vapour pressure at surface temperature T_s and e_w^* is saturated vapour pressure at a hypothetical wet surface temperature T_w, $\gamma = 0.665 \times 10^{-3}P$ (Allen *et al* 1998) is the psychrometric constant (kPa °C^{-1}) and P is atmospheric pressure (kPa). Notedly, the surface air temperature (T_s and T_w) were used in the absence of available surface temperature data. The saturated vapour pressure (unit of kPa) at temperature T is estimated following Allen *et al* (1998) as:

$$e^*(T) = 0.6108\exp\left(\frac{17.27T}{T+237.3}\right) \tag{4}$$

Assuming that the net radiation remains constant as the surface wetness changes, the change in sensible heat flux (H) is opposite to the change in latent heat flux (LE) based on the energy balance, so that (Granger 1989, Aminzadeh *et al* 2016):

$$\frac{\partial H}{\partial LE} = -1 = \gamma\frac{T_w - T_s}{e_w^* - e_s} \tag{5}$$

where e_s is the actual vapor pressure. T_w is the only unknown in equation (5), so it can be solved and further substituted into equation (3) to estimate the parameter b.

In this study, ET_p (mm d^{-1}) is estimated using the approach proposed by Penman (1948):

$$ET_p = \frac{0.408\Delta(T_s)(R_n - G)}{\Delta(T_s)+\gamma} + \frac{\gamma f(U_2)\,e_s^*(1-RH)}{\Delta(T_s)+\gamma} \tag{6}$$

where $\Delta(T_s)$ is the slope of the saturation vapor pressure curve at air temperature T_s (kPa °C^{-1}) (Allen *et al* 1998); R_n and G are net radiation and soil heat flux (MJ m^{-2} d^{-1}); RH is relative humidity; $f(U_2)$ (mm d^{-1} kPa^{-1}) is an empirical wind function to characterize the aerodynamic conditions of the atmosphere (Penman 1948), and it is defined as:

$$f(U_2) = 2.6\,(1 + 0.54U_2) \tag{7}$$

where U_2 is the wind speed (m s^{-1}) at a height of 2 m.

Based on the concept of equilibrium evapotranspiration defined by Bouchet (1963), ET_w (mm d^{-1}) is mostly a function of available energy and can be approximated with the Bowen ratio of a wet environment (β_{wet}) based on the energy-budget equation:

$$ET_w = \frac{0.408\,(R_n - G)}{1 + \beta_{wet}} \tag{8}$$

Similar to equation (5), the β_{wet} for the hypothetical wet environment from temperature T_w to T_s is:

$$\beta_{wet} = \frac{\partial H}{\partial LE} = \gamma\frac{T_s - T_w}{e_s^* - e_w^*} \tag{9}$$

It is worth to note that there is no necessity to calibrate any parameter in this improved CR formulation, whose accuracy was further verified in this study (see section 1 in Supplementary Information for details).

2.3. Data sets

The FLUXNET2015 Dataset (see section 2 in Supplementary Information for details) was used to evaluate the influence of RH on ET, and the performance of the improved CR formulation at site-level and weekly time scale. ERA-Interim meteorological data (Berrisford *et al* 2011) have been extensively used and verified for accuracy across the globe (Albergel *et al* 2013, Dee *et al* 2014, Vuichard and Papale 2015). To estimate global terrestrial ET ($ET_{CR\_ERA\text{-}Interim}$), input data to the improved CR formulation were obtained from gridded monthly ERA-Interim data over the 1979–2017 period (see section 3 in Supplementary Information for details). The spatial resolution of ERA-Interim data is approximately 0.7 degrees in longitude and latitude. Since such coarse spatial scale did not completely match the site-level FLUXNET2015 data, a dataset of the multi-year annual average basin-level ET was obtained and used as an additional independent observation to further verify the accuracy of $ET_{CR\_ERA\text{-}Interim}$ at a different spatial scale. In this study, 236 basins with long time series data (≥9 years) were selected (figure S3, see section 4 in supplementary information for details) (available online at stacks.iop.org/ERL/15/094066/mmedia). To reduce the uncertainty in selecting the soil moisture dataset, three widely used datasets were analysed, including the root-zone ERA-Interim soil moisture dataset (Berrisford *et al* 2011), the root-zone soil moisture dataset from Global Land Data Assimilation System (GLDAS) (Beaudoing and Rodell 2016) and the satellite-based surface soil moisture dataset released

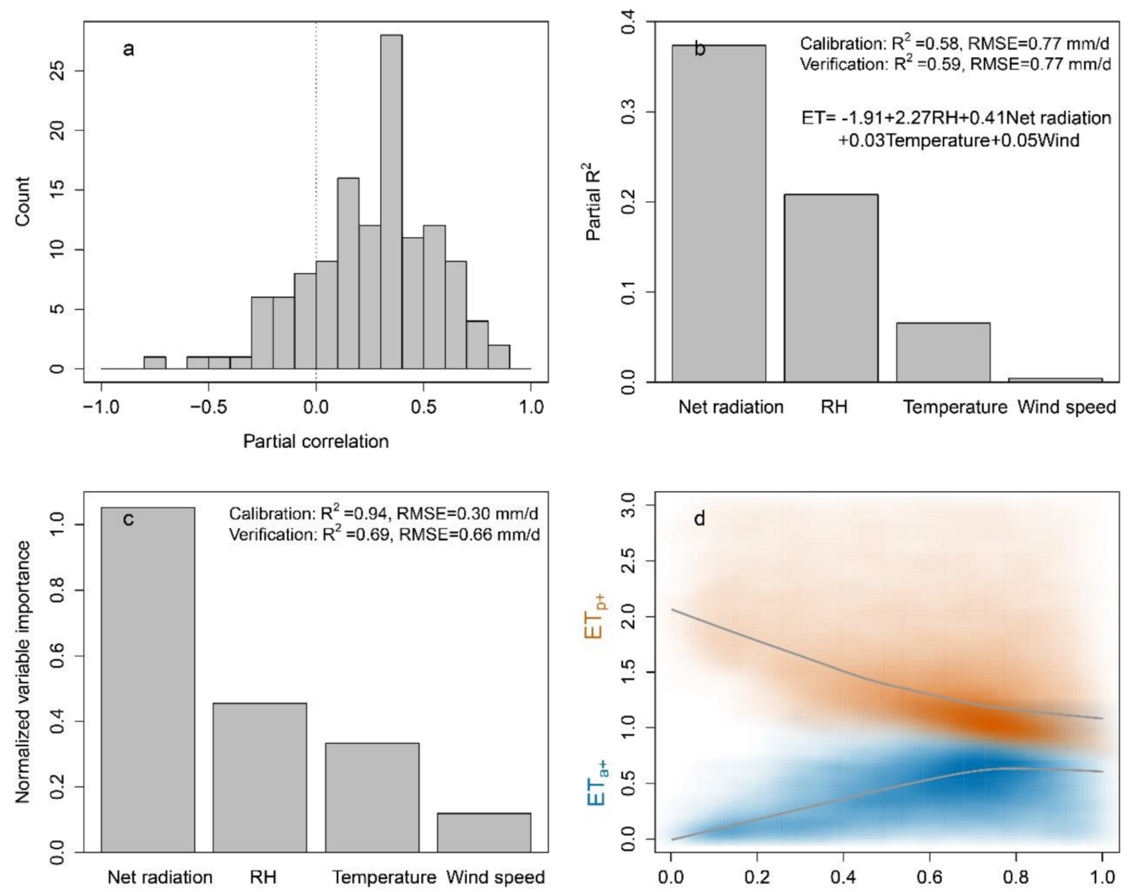

Figure 1. Influence of RH on ET according to weekly data from 127 eddy covariance sites: (a) histogram of partial correlation between RH and actual ET when impacts of net radiation, air temperature and wind speed were excluded, (b) the amount of unique variance (partial R^2) that each variable explains in multiple regression, (c) relative importance of factors affecting ET based on the normalized permutation-based variable importance in Random Forest, (d) smoothed scatter plot of normalized actual ET and potential ET vs RH for all of the sites.

by European Space Agency, Climate Change Initiative (ESA-CCI) (Liu *et al* 2012, Dorigo *et al* 2017) (see section 5 in supplementary information for details).

3. Results and discussion

3.1. Contribution of RH to ET based on observation data

127 eddy covariance sites (table S2) selected from the FLUXNET2015 dataset were used to analyse the contribution of RH to ET. Partial correlation analysis (Kim 2015) indicated that 104 of 127 sites showed a positive correlation between RH and ET when the impacts of net radiation, air temperature, and wind speed were excluded (figure 1(a)), and the positive correlation dominated in all 12 vegetation cover types or biomes except permanent wetlands where actual ET is close to potential ET (figure S5). Based on the weekly data from all of the 127 eddy covariance sites, the multiple regression and Random Forest methods were used to evaluate the relative importance of net radiation, temperature, RH, and wind speed in controlling ET. As expected, net radiation resulted in the most important driver of ET representing the energy source for ET itself (figures 1(b) and (c)). However, both the multiple regression and Random Forest methods indicated that RH is a more important driver than temperature (figures 1(b) and (c)) highlighting its importance especially since a sharp decrease in RH has been widely observed at global scale in recent years (Simmons *et al* 2010, Willett *et al* 2014). The positive partial correlation (figure 1(a)) and positive slope of RH vs ET in multiple regression (figure 1(b)) are consistent with the evidence that plants close their stomata to prevent excessive water loss in response to increasing atmospheric VPD (Mcadam and Brodribb 2015). Because the relationship between RH and ET may be nonlinear, a scatter plot of dimensionless ET and RH was used to illustrate their relationship (see section 6 in the supplementary information for details on the method used to obtain dimensionless ET). The scatter plot of RH in relation to the normalized measured actual ET and estimated potential ET (refer to equation (6) for details on the estimation method) illustrates that the normalized actual ET generally increased with increasing RH, while the normalized potential ET generally decreased with increasing RH (figure 1(d)). This relationship is consistent with the framework of Bouchet (1963), who identified the complementary relationship between

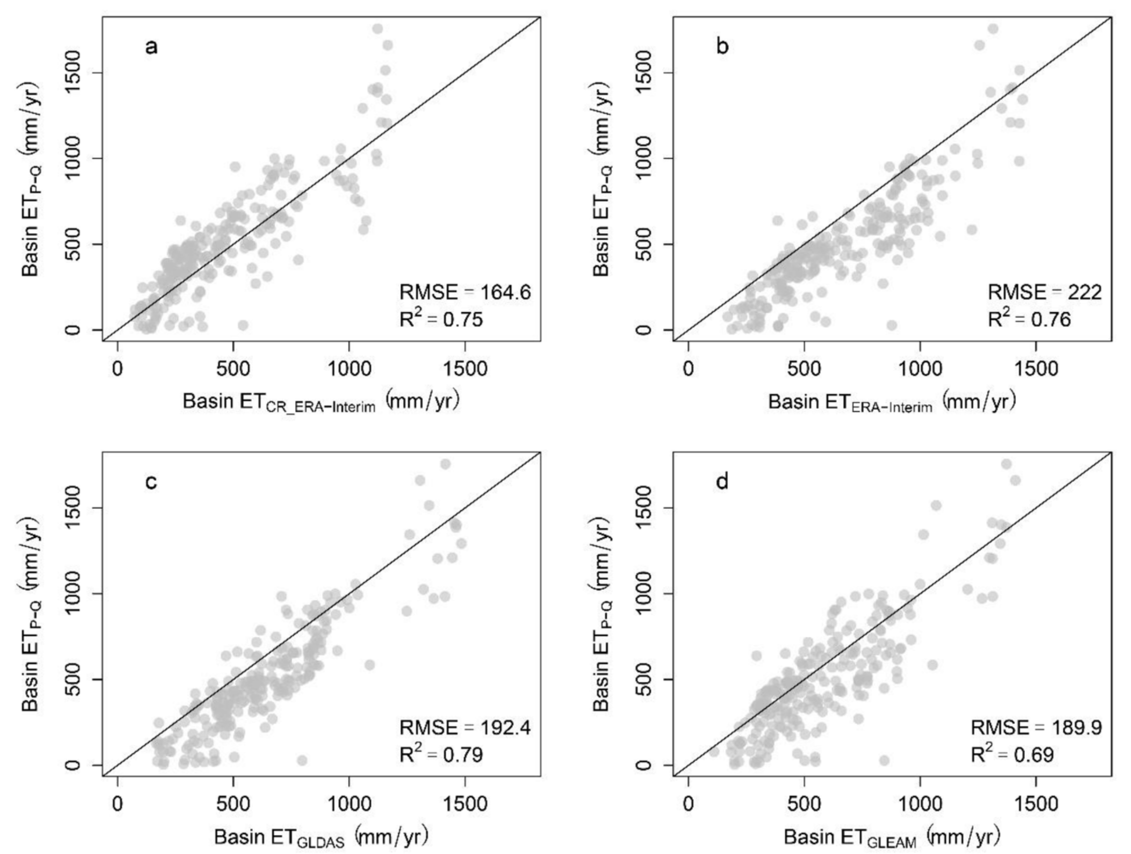

Figure 2. Validation of different simulated actual ET based on the basin-level multi-year annual average actual ET (ET_{P-Q}), where (a) for actual ET estimated using the CR formulation based on the ERA-Interim meteorological forcing data ($ET_{CR\_ERA-Interim}$), (b) for actual ET obtained from ERA-Interim ($ET_{ERA-Interim}$), (c) for actual ET obtained from GLDAS (ET_{GLDAS}), and (d) for actual ET obtained from GLEAM (ET_{GLEAM}).

actual and potential ET stating that the fraction of energy not used for evapotranspiration is dissipated as increased sensible heat flux that in turn increases potential ET.

3.2. Performance of improved CR formulation in estimating ET

No parameter calibration is required in the improved CR formulation, thus strongly facilitating its application on a global scale. The performance of the improved CR formulation was compared with other commonly adopted CR formulations against the FLUXNET2015 Dataset. Results indicated that the RMSE of the estimated actual ET generally decreased from 1.32 mm d^{-1}, 1.56 mm d^{-1} and 1.7 mm d^{-1} to 0.89 mm d^{-1} when the improved CR formulation was used instead of the other commonly adopted CR formulations (figure S1, see section 1 in supplementary information for details). The calibrated data-driven methods (i.e. multiple regression and Random Forest methods in figures 1(b) and (c)) performed slightly better than the improved CR formulation in estimating ET in terms of RMSE. However, the application of methods requiring parameter calibration is limited in data-scarce regions, hence only the CR formulation not requiring any parameter adjustment was considered in this study to estimate global terrestrial ET.

Using the required meteorological forcing data for CR formulations from ERA-Interim data, the global terrestrial ET ($ET_{CR\_ERA-Interim}$) over the 1979–2017 period was estimated. Compared to other widely used ET data derived from ERA-Interim, GLDAS (Rodell *et al* 2004, Beaudoing and Rodell 2016) and Global Land Evaporation Amsterdam Model (GLEAM) (Miralles *et al* 2011, Martens *et al* 2017), results show that the basin-level ET estimated by $ET_{CR\_ERA-Interim}$ outperforms the other methods by approximately 25.9%, 14.4% and 13.3% (as reductions in RMSE), respectively (figure 2), confirming the overall reliability of the $ET_{CR\_ERA-Interim}$ proposed in this study.

3.3. Change in RH from 1979-2017

Changes in RH trends were assessed using the ERA-Interim meteorological data. A piecewise linear regression method was used to assess the changes in the RH trends and detect the presence of mutation points (Muggeo 2003). We found that RH exhibited a slightly increasing trend before 1998 but started to decrease sharply afterwards (figure 3(a)). A decrease in RH was observed over approximately 68%

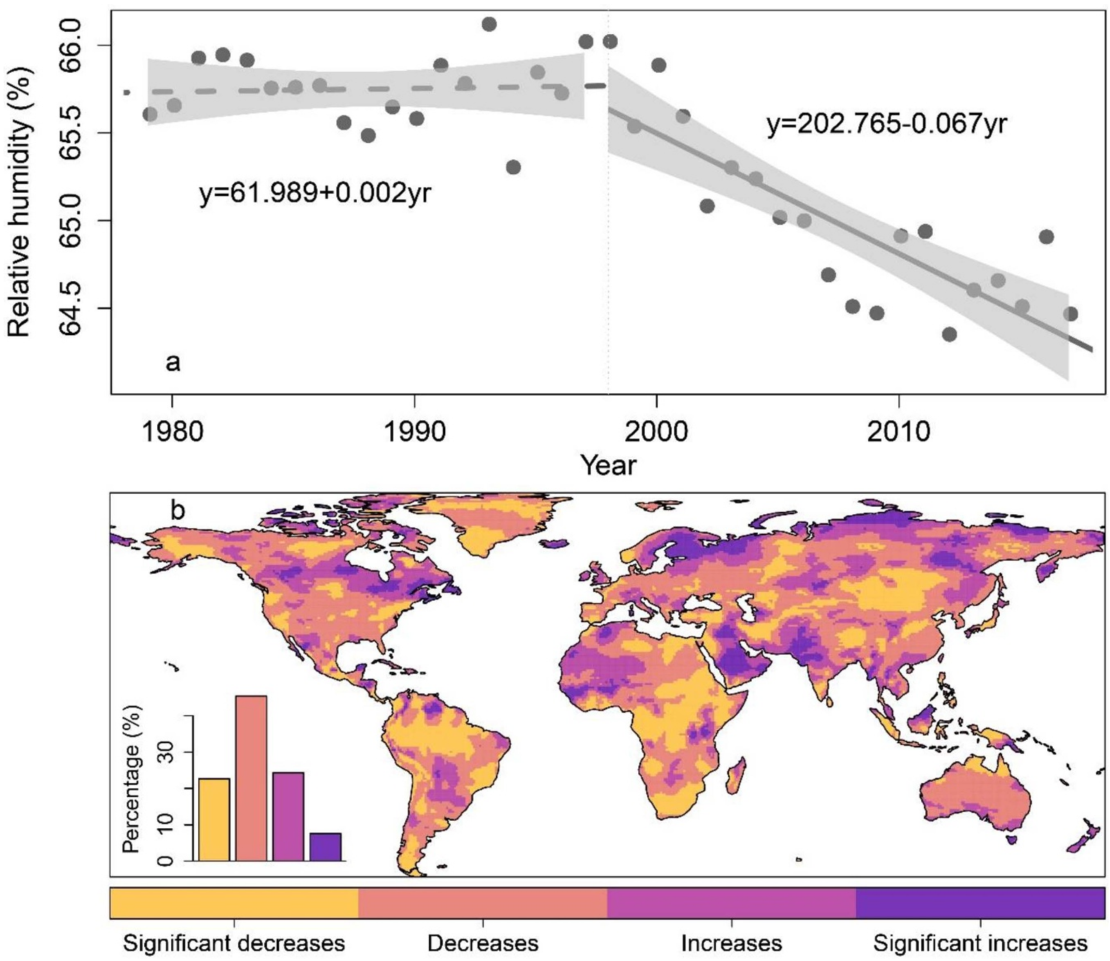

Figure 3. Spatiotemporal variations in relative humidity (RH), (a) piecewise linear regression of the global average RH, (b) map of the linear trend of the annual average RH for the period 1998–2017. The solid line in (a) indicates that the linear trend is significant at the 5% significance level, and the shaded areas represent the 95% confidence interval.

of the land (except Antarctica), especially in northern parts of South America, central parts of Africa and Asia (figure 3(b)). In contrast with the expectation that reduced RH would mainly occur in arid regions where soil drying can suppress ET and reduce RH, we also observed reductions in humid regions (figure S6). Byrne and Gorman (2016) stated that this reduction was related to the relatively greater warming over land than ocean. Thus, the specific humidity of air advected from the ocean to land increased less than the increase in saturation-specific humidity over land.

3.4. Change in global terrestrial ET from 1979-2017 and its main driver

The spatiotemporal variations in ET from 1979–2017 based on $ET_{CR\_ERA\text{-}Interim}$ revealed that global terrestrial annual average ET increased before 1998 and slightly decreased after 1998 (figure 4(a)). A decline in the trend of global terrestrial ET from 1998–2000 until 2008 was also found by Jung *et al* (2010) using a data-driven method based on FLUXNET data. The approach proposed here further supports a decline in the global average terrestrial ET since 1998 that extended until 2017. At the regional scale, different trends of annual average ET were obtained (figure 4(b)). From 1998 to 2017, approximately half of the land (excluding Antarctica) was dominated by decreased annual ET, and even more regions with reduced increasing rates of annual ET covered approximately 58% of the land surface (figure 4(c)). The decreased annual ET was more significant in arid regions (figure S7).

Before 1998, RH remained almost constant (figure 3(a)); thus, the terrestrial ET was generally energy limited, and the ET increased with increasing temperatures (figure S8). Afterwards, RH decreased implying an increased VPD (figure S9) inducing the closure of plant stomata (Mcadam and Brodribb 2015). Novick *et al* (2016) found that VPD limits ET to a greater extent than soil water stress in many biomes. Hence, the overall reduction in terrestrial ET after 1998 was considered to be mostly caused by reduced RH, which induced plant stomatal regulation to prevent excessive water loss. Notedly, this explanation is based on leaf-level (micro-scale) dynamic, that may not entirely transfer at canopy level since a fraction of canopy evaporation is made

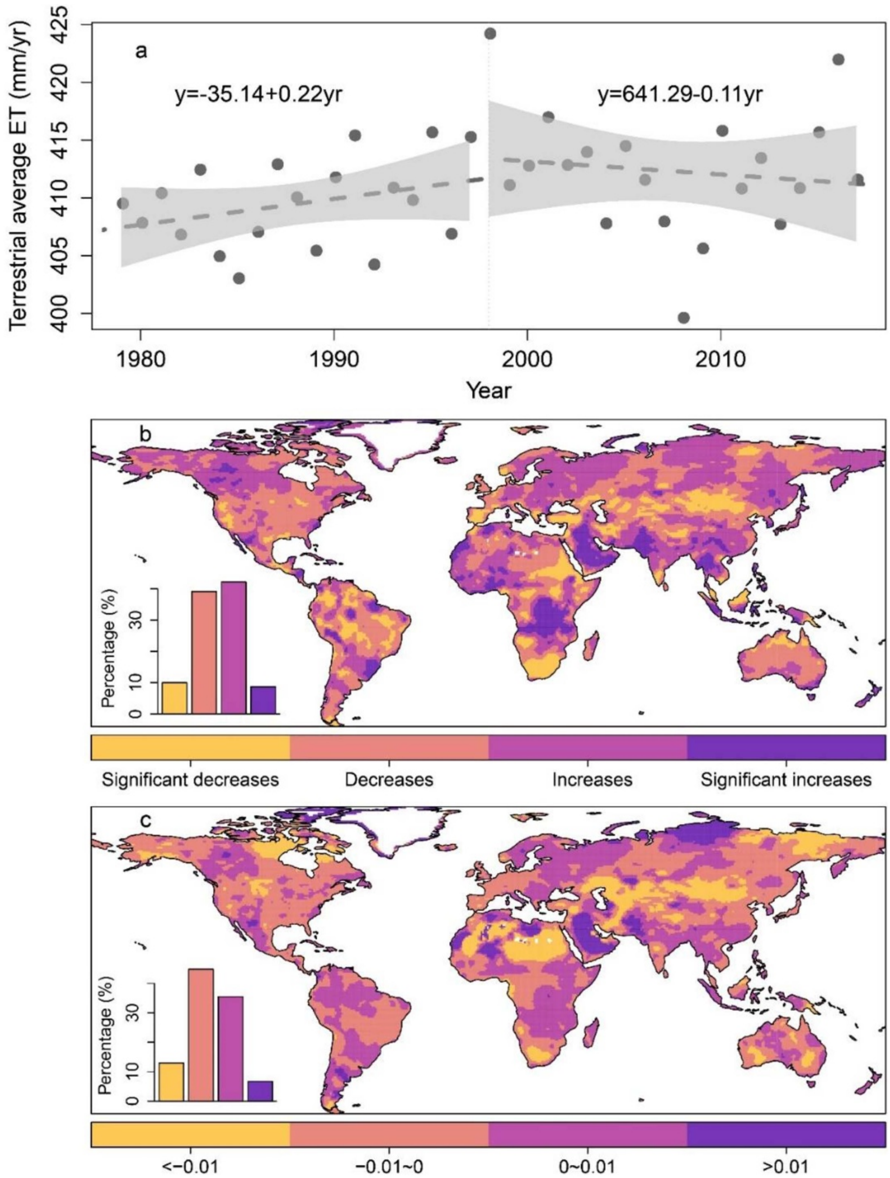

Figure 4. Spatiotemporal variations in terrestrial annual actual ET, (a) piecewise linear regression of global average terrestrial annual actual ET, (b) spatial pattern of the linear trend of the annual actual ET for the period 1998–2017, (c) spatial pattern of the differences in the linear trend of annual actual ET between 1979–1997 and 1998–2017. Trends were scaled by the corresponding multi-year annual average actual ET. The dashed lines in (a) indicate that the linear trend was not significant at the 5% significance level, and the shaded areas represent the 95% confidence interval.

by evaporation from the soil and/or other wet surfaces (Perez-Priego *et al* 2018). Therefore, we estimated both canopy conductance (G_s) and leaf-level stomatal conductance (g_s) and verified whether the variation of normalized G_s is consistent with g_s. By inverting the Penman-Monteith equation (Allen *et al* 1998), we computed the canopy-level G_s (see section 8 in supplementary information for details). Results showed that the G_s indeed sharply decreased after 1998 (figure 5). Since increasing atmospheric CO_2 is also known to stimulate stomatal closure (Ainsworth and Rogers 2007), to disentangle the role of atmospheric CO_2 concentration and RH in reducing G_s, we applied the linearized optimal stomatal control model (OptiL) (Katul *et al* 2010) to approximate the relative variations in leaf-level g_s (see section 9 in supplementary information for details). It was expected that the relative variations in normalized G_s and g_s would remain similar when the regulation of G_s was exclusively through stomatal control (Rigden and Salvucci 2017). Figure 5 shows that the relative variations in normalized G_s and g_s are highly correlated, and the reduced G_s is largely controlled by the decreased RH (i.e. increased VPD). This result highlights the critical role of the stomatal response to decreased RH in modulating the transfer of moisture to the atmosphere. Nevertheless, atmospheric demand represents only one of the key constraints to stomata regulation. Further observations are needed to quantify the present and future role of other resistances to atmospheric demand: the soil (Carminati and Javaux 2020) and the xylem (Eller *et al* 2020).

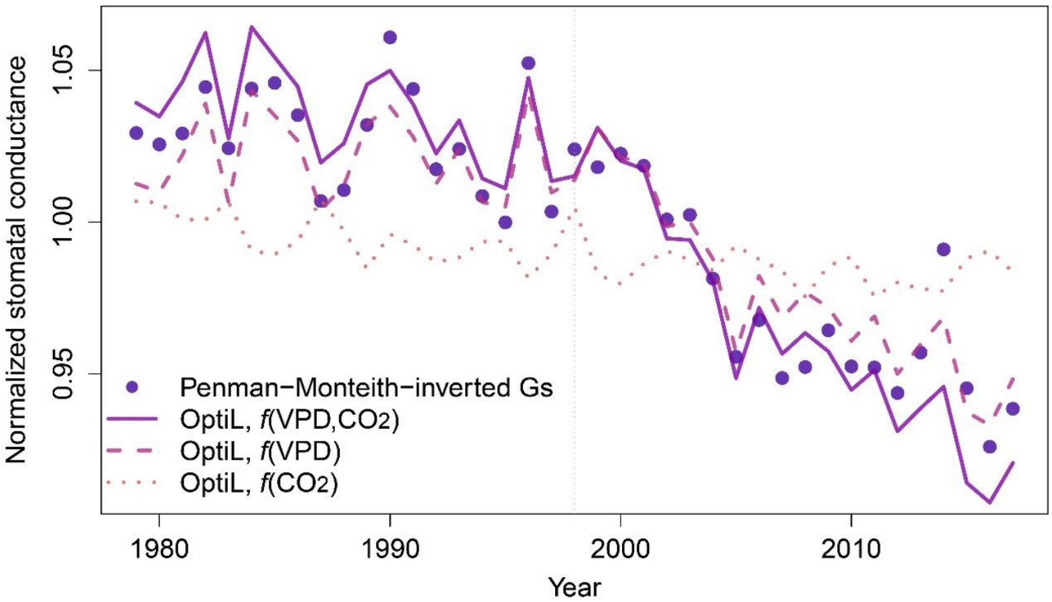

Figure 5. Temporal evolution of the normalized Penman-Monteith-inverted G_s and OptiL g_s, where $f(.)$ indicates with or without dynamic CO_2 and VPD in the OptiL model.

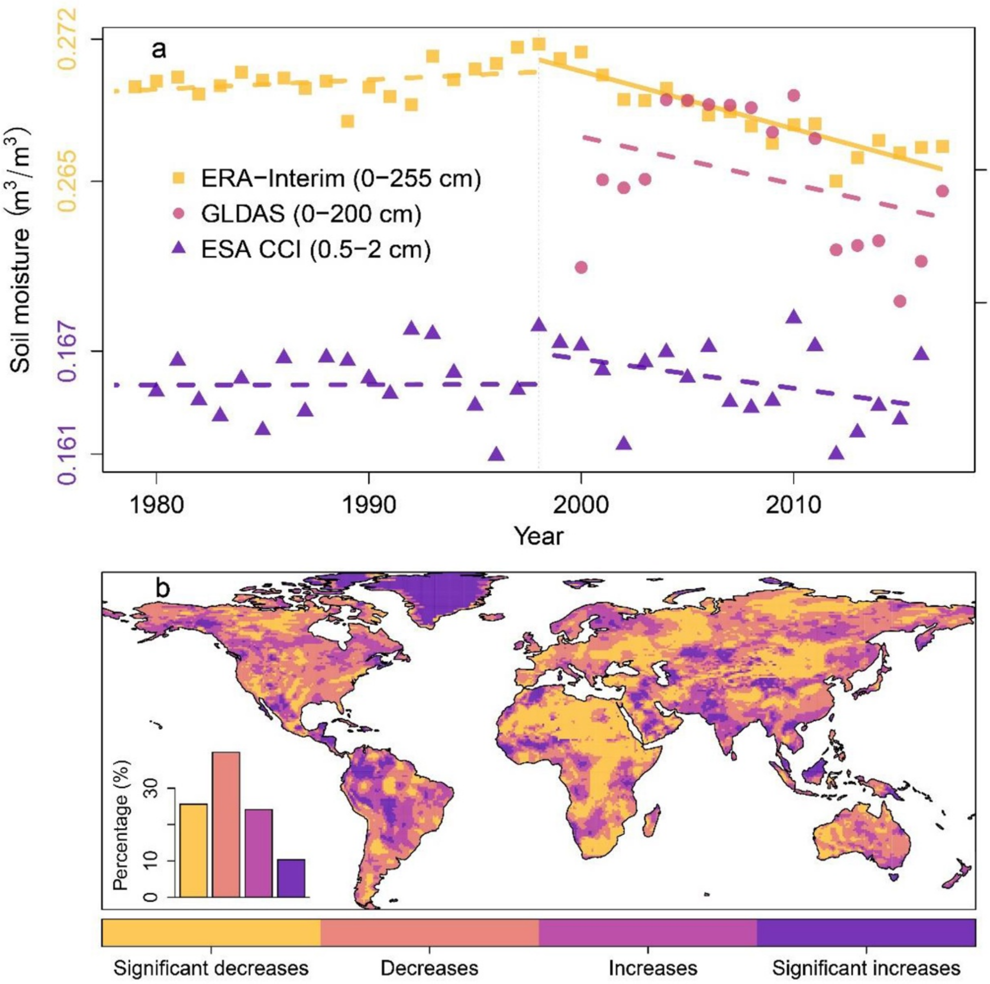

Figure 6. Spatiotemporal variations in soil moisture, (a) temporal evolution of global average soil moisture obtained from different datasets, (b) map of the linear trend of annual average soil moisture obtained from ERA-Interim for the period 1998–2017. For (a), the solid line indicates that the linear trend is significant at the 5% significance level.

3.5. Discussion

Although we have attributed reduced ET to stomatal regulation, we must also consider that wide regions exist on the Earth without or poorly covered by vegetation. ET is dominated by soil evaporation in some arid regions, such as deserts in Sahara and central Asia (Zhang *et al* 2016). Here, figure 6(a) shows that the global average surface soil moisture also significantly decreased after 1998 based on the data from GLDAS, ERA-Interim and ESA CCI (Liu *et al* 2012, Dorigo *et al* 2017, Gruber *et al* 2017). The reduction in root-zone (or 0–255 cm soil depth) soil moisture occurred widely across the globe, especially in most parts of Africa, Australia and Europe (figure 6(b)). Thus, soil drying further suppresses both soil evaporation and plant evapotranspiration, and a continued global soil drying is expected in the future (Gu, *et al* 2019).

The start time of RH reduction was consistent with the beginning of warming hiatus around 1998, while such RH reduction did not terminate with the end of warming hiatus around 2012 (Medhaug *et al* 2017). According to ET reduction shown here (figure 4), decreased energy exchange as ET would result in increased energy exchange as sensible heat flux, accelerating warming over the land surface (Vogel *et al* 2017). This mechanism may therefore have contributed to the end of the warming hiatus itself, however such a connection needs to be further analysed and demonstrated. Besides, the continued greater warming over land than the ocean enhances the faster increase in saturation specific humidity over land, leading to further reduced RH (Byrne and O'Gorman 2016), therefore representing a positive feedback between decreased ET and reduced RH. Another positive feedback mechanism exists between reduced RH and soil drying, and the concurrent soil drying and atmospheric aridity (low RH) are found to be greatly exacerbated by land-atmosphere feedbacks (Zhou *et al* 2019). Reduced RH (i.e. rising VPD) has been considered as a major contributor in recent drought-induced plant mortality (Grossiord *et al* 2020), making plant adaptation and species change in response to a decline in RH worth of future attention.

4. Conclusions

Our results indicate that global terrestrial ET is not increasing since 1998 due to the reduction of available water in the soil-vegetation-atmosphere continuum. We found that the decreased atmospheric RH cancelled the increase in the global terrestrial ET observed until 1998. Physically, the decreased RH induced plant water stress and triggered stomatal closure to prevent excessive water loss. Terrestrial ET is the main source of precipitation on the land surface and a key driver of the intensified water cycle under global warming (Huntington 2006, Donat *et al* 2016). The continuing decrease in terrestrial ET observed here indicates that the ongoing temperature-driven acceleration of the terrestrial water cycle is getting constrained due to terrestrial vegetation feedbacks. Nevertheless, further research is needed to disentangle the complexity of vegetation-soil-atmosphere interactions in the climate system.

Acknowledgments

This work used FLUXNET data acquired and shared by the global FLUXNET community, including AmeriFlux, AfriFlux, AsiaFlux, CarboAfrica, CarboEuropeIP, CarboItaly, CarboMont, ChinaFlux, Fluxnet-Canada, GreenGrass, ICOS, KoFlux, LBA, NECC, OzFlux-TERN, Swiss FluxNet, TCOS-Siberia, and USCCC. The ERA-Interim reanalysis data obtained from ECMWF and processed by LSCE. The FLUXNET eddy covariance data processing and harmonization was carried out by the European Fluxes Database Cluster, AmeriFlux Management Project, and Fluxdata project of FLUXNET, with the support of CDIAC and ICOS Ecosystem Thematic Center, and the OzFlux, ChinaFlux and AsiaFlux offices. In detail, US-Prr is supported by JAMSTEC and IARC/UAF collaboration study and Japanese Arctic Research Program (ArCS); Department of Energy Office of Science, Ameriflux Network Management Project Support for UW ChEAS Cluster (US-Los, US-PFa, US-WCr, US-Syv, 2012-present). CPC Global Unified Precipitation data was provided by the NOAA/OAR/ESRL PSD, Boulder, Colorado, USA, from their Web site at https://www.esrl.noaa.gov/psd/data/gridded/. Monthly GRDC Reference Dataset was provided by the Global Runoff Data Centre, 56068 Koblenz, Germany. The multi-satellite surface soil moisture data was provided by ESA CCI SM project. The authors acknowledge contributions from individual researcher who made sincere efforts to gather these data sets and made them available for synthesis work. The work was supported by National Key R&D Program of China (2016YFC0402706, 2016YFC0402710); the National Natural Science Foundation of China (51909057, 51539003, 41901041); China Postdoctoral Science Foundation (2017M610292). MG acknowledges funding by Swiss National Science Foundation project ICOS-CH Phase 2 20FI20_173691. The authors also acknowledge Professor Changliang Shao, Dr. Mika Aurela for their interest and helpful correspondence. Finally, we thank two anonymous reviewers and the Editorial Board Member for their constructive comments and review of the manuscript.

Data availability statements

The data that support the findings of this study are available from the corresponding author upon reasonable request. The FLUXNET2015 dataset is available from the global FLUXNET community website (https://fluxnet.fluxdata.org/data/fluxnet2015-dataset/); the multi-satellite surface soil moisture data are available from the ESA CCI SM project website (https://www.esa-soilmoisture-cci.org/); ERA-Interim datasets are available from the NCAR Research Data Archive at https://rda.ucar.edu/datasets/ds627.1/; GLDAS datasets are available from the NASA Goddard Earth Sciences (GES) Data and Information Services Center (DISC) at https://disc.gsfc.nasa.gov/datasets?keywords=GLDAS; GLEAM datasets are available from https://www.gleam.eu/.

ORCID iDs

Mingzhong Xiao https://orcid.org/0000-0002-9462-2577
Leonardo Montagnani https://orcid.org/0000-0003-2957-9071
Nina Buchmann https://orcid.org/0000-0003-0826-2980
Sebastian Wolf https://orcid.org/0000-0001-7717-6993
Beniamino Gioli https://orcid.org/0000-0001-7631-2623

References

Albergel C *et al* 2013 Skill and global trend analysis of soil moisture from reanalyses and microwave remote sensing *J. Hydrometeorol.* **14** 1259–77
Allen R G, Pereira L S, Raes D and Smith M 1998 Crop evapotranspiration —guidelines for computing crop water requirements *FAO Irrigation and Drainage Paper 56* (Rome: Food and Agriculture Organization)
Aminzadeh M, Roderick M L and Or D 2016 A generalized complementary relationship between actual and potential evaporation defined by a reference surface temperature *Water Resour. Res.* **52** 385–406
Ainsworth E A and Rogers A 2007 The response of photosynthesis and stomatal conductance to rising [CO2]: mechanisms and environmental interactions *Plant Cell Environ.* **30** 258–70
Beaudoing H and Rodell M 2016 *GLDAS Noah Land Surface Model L4 Monthly 0.25 × 0.25 Degree V2.1* NASA/GSFC/HSL: (Greenbelt, Maryland: Goddard Earth Sciences Data and Information Services Center) (Accessed: April 2018) (https://doi.org/10.5067/SXAVCZFAQLNO)
Berrisford P *et al* 2011 The ERA-interim archive version 2.0 ECMWF, Shinfield Park, Reading
Bouchet R J 1963 Évapotranspiration réelle evapotranspiration potentielle, signification climatique *IAHS Publ.* **62** 134–42
Breiman L 2001 Random Forests *Mach. Learn.* **45** 5–32
Brutsaert W 2015 A generalized complementary principle with physical constraints for land-surface evaporation *Water Resour. Res.* **51** 8087–93
Burke M *et al* 2018 Higher temperatures increase suicide rates in the United States and Mexico *Nat. Clim. Change* **8** 723–9
Byrne M P and O'Gorman P A 2016 Understanding decreases in land relative humidity with global warming: conceptual model and GCM simulations *J. Clim.* **29** 9045–61
Carminati A and Javaux M 2020 Soil rather than xylem vulnerability controls stomatal response to drought *Trends Plant Sci.* **25** 868–80
Dai A 2006 Recent climatology, variability, and trends in global surface humidity *J. Clim.* **19** 3589–606
Dee D P *et al* 2014 Toward a consistent reanalysis of the climate system *Bull. Am. Meteorol. Soc.* **95** 1235–48
Donat M G, Lowry A L, Alexander L V, O'Gorman P A and Maher N 2016 More extreme precipitation in the world's dry and wet regions *Nat. Clim. Change* **6** 508–13
Dorigo W *et al* 2017 ESA CCI soil moisture for improved earth system understanding: state-of-the art and future directions *Remote Sens. Environ.* **203** 185–215
Eller C B *et al* 2020 Stomatal optimization based on xylem hydraulics (SOX) improves land surface model simulation of vegetation responses to climate *New Phytol.* **226** 1622–37
Granger R J 1989 A complementary relationship approach for evaporation from nonsaturated surfaces *J. Hydrol.* **111** 31–38
Grömping U 2009 Variable importance assessment in regression: linear regression versus random forest *Am. Stat.* **63** 308–19
Grossiord C *et al* 2020 Plant responses to rising vapor pressure deficit *New Phytol.* **226** 1550–66
Gruber A, Dorigo W A, Crow W and Wagner W 2017 Triple collocation-based merging of satellite soil moisture retrievals *IEEE Trans. Geosci. Remote Sens.* **55** 6780–92
Gu X *et al* 2019 Attribution of global soil moisture drying to human activities: a quantitative viewpoint *Geophys. Res. Lett.* **46** 2573–82
Huntington J L, Szilagyi J, Tyler S W and Pohll G M 2011 Evaluating the complementary relationship for estimating evapotranspiration from arid shrublands *Water Resour. Res.* **47** W05533
Huntington T G 2006 Evidence for intensification of the global water cycle: review and synthesis *J. Hydrol.* **319** 83–95
Jung M *et al* 2010 Recent decline in the global land evapotranspiration trend due to limited moisture supply *Nature* **467** 951
Kahler D M and Brutsaert W 2006 Complementary relationship between daily evaporation in the environment and pan evaporation *Water Resour. Res.* **42** W05413
Katul G, Manzoni S, Palmroth S and Oren R 2010 A stomatal optimization theory to describe the effects of atmospheric CO2 on leaf photosynthesis and transpiration *Ann. Bot.* **105** 431–42
Kim S 2015 ppcor: an R package for a fast calculation to semi-partial correlation coefficients *Commun. Stat. Appl. Methods* **22** 665–74
Liu Y Y *et al* 2012 Trend-preserving blending of passive and active microwave soil moisture retrievals *Remote Sens. Environ.* **123** 280–97
Martens B *et al* 2017 GLEAM v3: satellite-based land evaporation and root-zone soil moisture *Geosci. Model Dev.* **10** 1903–25
Mcadam S A M and Brodribb T J 2015 The evolution of mechanisms driving the stomatal response to vapor pressure deficit *Plant Physiol.* **167** 833–43
Medhaug I, Stolpe M B, Fischer E M and Knutti R 2017 Reconciling controversies about the 'global warming hiatus' *Nature* **545** 41–47
Miralles D G *et al* 2011 Global land-surface evaporation estimated from satellite-based observations *Hydrol. Earth Syst. Sci.* **15** 453–69
Muggeo V M R 2003 Estimating regression models with unknown break-points *Stat. Med.* **22** 3055–71
Novick K A *et al* 2016 The increasing importance of atmospheric demand for ecosystem water and carbon fluxes *Nat. Clim. Change* **6** 1023
Oki T and Kanae S 2006 Global hydrological cycles and world water resources *Science* **313** 1068–72
Penman H L 1948 Natural evaporation from open water, bare soil and grass *Proc. R. Soc. London, Ser. A* **193** 120–45
Perez-Priego O *et al* 2018 Partitioning eddy covariance water flux components using physiological and micrometeorological approaches *J. Geophys. Res.* **123** 3353–70
Rigden A J and Salvucci G D 2017 Stomatal response to humidity and CO2 implicated in recent decline in US evaporation *Glob. Change Biol.* **23** 1140–51
Rodell M *et al* 2004 The global land data assimilation system *Bull. Am. Meteorol. Soc.* **85** 381–94

Simmons A J, Willett K M, Jones P D, Thorne P W and Dee D P 2010 Low-frequency variations in surface atmospheric humidity, temperature, and precipitation: inferences from reanalyses and monthly gridded observational data sets *J. Geophys. Res.: Atmos.* **115** D1

Strobl C, Boulesteix A-L, Zeileis A and Hothorn T 2007 Bias in random forest variable importance measures: illustrations, sources and a solution *BMC Bioinform.* **8** 25

Szilagyi J and Jozsa J 2008 New findings about the complementary relationship-based evaporation estimation methods *J. Hydrol.* **354** 171–86

Trenberth K E, Fasullo J and Smith L 2005 Trends and variability in column-integrated atmospheric water vapor *Clim. Dyn.* **24** 741–58

Trenberth K E, Fasullo J T and Kiehl J 2009 Earth's global energy budget *Bull. Am. Meteorol. Soc.* **90** 311–23

Vicente-Serrano S M *et al* 2018 Recent changes of relative humidity: regional connections with land and ocean processes *Earth Syst. Dyn.* **9** 915–37

Vogel M M *et al* 2017 Regional amplification of projected changes in extreme temperatures strongly controlled by soil moisture-temperature feedbacks *Geophys. Res. Lett.* **44** 1511–9

Vuichard N and Papale D 2015 Filling the gaps in meteorological continuous data measured at FLUXNET sites with ERA-Interim reanalysis *Earth Syst. Sci. Data* **7** 157–71

Wang K and Dickinson R E 2012 A review of global terrestrial evapotranspiration: observation, modeling, climatology, and climatic variability *Rev. Geophys.* **50** Rg2005

Willett K M *et al* 2014 HadISDH land surface multi-variable humidity and temperature record for climate monitoring *Clim. Past* **10** 1983–2006

Willett K M, Jones P D, Gillett N P and Thorne P W 2008 Recent changes in surface humidity: development of the hadCRUH dataset *J. Clim.* **21** 5364–83

Wright M N and Ziegler A 2017 ranger: a fast implementation of random forests for high dimensional data in C++ and R *J. Stat. Softw.* **77** 1–17

Yuan W *et al* 2019 Increased atmospheric vapor pressure deficit reduces global vegetation growth *Sci. Adv.* **5** eaax1396

Zhang Y *et al* 2016 Multi-decadal trends in global terrestrial evapotranspiration and its components *Sci. Rep.* **6** 19124

Zhou S *et al* 2019 Land–atmosphere feedbacks exacerbate concurrent soil drought and atmospheric aridity *Proc. Natl Acad. Sci.* **116** 18848–53